

# Glycan Imaging in Intact Rat Hearts and Glycoproteomic Analysis Reveal the Upregulation of Sialylation during Cardiac Hypertrophy

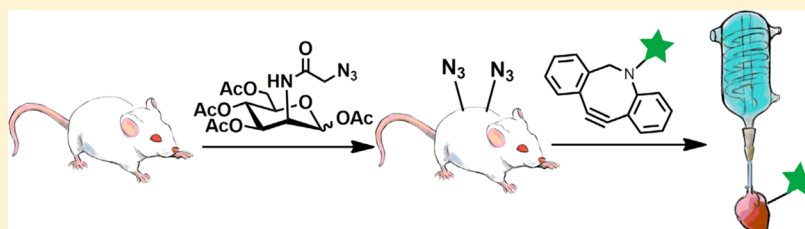
Jie Rong,<sup>†,⊥,▽</sup> Jing Han,<sup>‡,▽</sup> Lu Dong,<sup>†,||,▽</sup> Yanhong Tan,<sup>†</sup> Huaqian Yang,<sup>‡</sup> Lianshun Feng,<sup>†,⊥</sup> Qi-Wei Wang,<sup>‡</sup> Rong Meng,<sup>†,||</sup> Jing Zhao,<sup>\*,⊥,#</sup> Shi-Qiang Wang,<sup>\*,‡</sup> and Xing Chen<sup>\*,†,§,||</sup>

<sup>†</sup>Beijing National Laboratory for Molecular Sciences, Key Laboratory of Bioorganic Chemistry and Molecular Engineering of Ministry of Education, College of Chemistry and Molecular Engineering, <sup>‡</sup>State Key Laboratory of Biomembrane and Membrane Biotechnology, College of Life Sciences, <sup>§</sup>Synthetic and Functional Biomolecules Center, and <sup>||</sup>Peking-Tsinghua Center for Life Sciences, Peking University, Beijing 100871, China

<sup>⊥</sup>School of Chemical Biology and Biotechnology, Shenzhen Graduate School of Peking University, Shenzhen 518055, China

<sup>#</sup>State Key Laboratory of Pharmaceutical Biotechnology, School of Life Sciences, Institute of Chemistry and Biomedical Sciences, Nanjing University, Nanjing 210093, China

**S** Supporting Information



**ABSTRACT:** In the heart, glycosylation is involved in a variety of physiological and pathological processes. Cardiac glycosylation is dynamically regulated, which remains challenging to monitor *in vivo*. Here we describe a chemical approach for analyzing the dynamic cardiac glycome by metabolically labeling the cardiac glycosylated proteins with azides, serving as a chemical reporter, are chemoselectively conjugated with fluorophores using copper-free click chemistry for glycan imaging; derivatizing azides with affinity tags allows enrichment and proteomic identification of glycosylated cardiac proteins. We demonstrated this methodology by visualization of the cardiac sialylated glycosylated proteins in intact hearts and identification of more than 200 cardiac proteins modified with sialic acids. We further applied this methodology to investigate the sialylation in hypertrophic hearts. The imaging results revealed an increase of sialic acid biosynthesis upon the induction of cardiac hypertrophy. Quantitative proteomic analysis identified multiple sialylated proteins including neural cell adhesion molecule 1, T-kininogens, and  $\alpha_2$ -macroglobulin that were upregulated during hypertrophy. The methodology may be further extended to other types of glycosylation, as exemplified by the mucin-type O-linked glycosylation. Our results highlight the applications of metabolic glycan labeling coupled with bioorthogonal chemistry in probing the biosynthesis and function of cardiac glycome during pathophysiological responses.

## INTRODUCTION

Mammalian glycan structures vary in different tissues,<sup>1</sup> and glycosylation is tightly regulated during development and disease progression.<sup>2,3</sup> The cardiac glycome, defined as the complete set of glycans in hearts, is dynamically remodeled, which modulates cardiac functions.<sup>4,5</sup> Accumulating evidence indicates that many cardiac ion channels are glycosylated with N-linked glycans, mucin-type O-linked glycans, and sialic acids, which are vital for regulating cardiac electrical signaling and heart rhythm.<sup>6–12</sup> Aberrant cardiac glycosylation has been implicated in pathological states such as hypertrophy, heart failure, and congenital disorders.<sup>13–16</sup>

Probing cardiac glycosylation has mostly relied on biochemical analysis of purified glycans and glycoproteins and glycome expression profiling. For *in vivo* studies in animal models, which are critical for cardiovascular diseases, knockout

of glycosyltransferase genes has been most commonly used. However, direct visualization of cardiac glycosylation in intact hearts remains a challenging task. This obstacle undermines investigations that seek to resolve the spatial distribution of glycans within the heart tissues or to monitor the dynamic changes of cardiac glycosylation under physiological and pathological conditions. The significance of performing such experiments is underlined by the dynamic changes of glycosylation in response to pathophysiological stimuli from the tissue microenvironment.<sup>2,3,17</sup> Although traditionally regarded as a relatively quiescent organ, the adult mammalian heart undergoes dynamic metabolism<sup>18</sup> and more recently has been shown to possess reparative capability.<sup>19</sup>

Received: August 19, 2014

Published: October 14, 2014

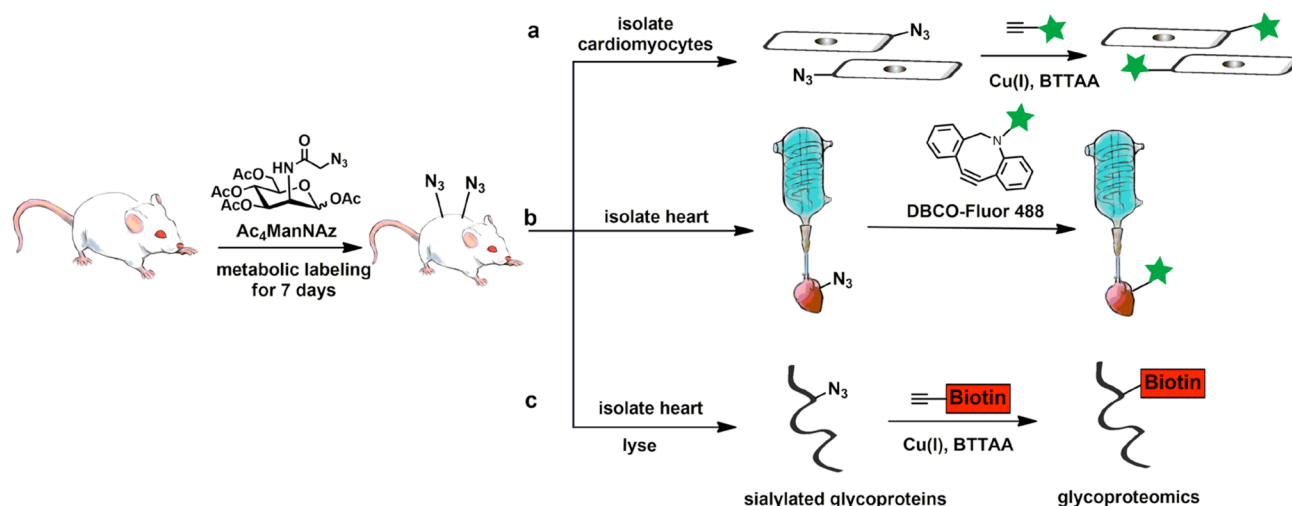


**Figure 1.** *In vivo* metabolic glycan labeling enables visualization of cardiac sialome and proteomic identification of cardiac sialylated proteins. Living rats are injected intraperitoneally with  $\text{Ac}_4\text{ManNAz}$ , which is metabolically incorporated into cell-surface sialylated glycans. The azides then serve as a chemical reporter for glycan imaging and glycoprotein enrichment and identification by means of bioorthogonal chemistry. (a) The cardiomyocytes are acutely isolated, followed by reaction with alkyne-Fluor 488 and confocal fluorescence imaging at the cellular level. (b) The azide-incorporated hearts are isolated and perfused on the Langendorff system. The bioorthogonal labeling is performed at the organ level by perfusing DBCO-Fluor into the hearts, followed by confocal fluorescence imaging of the intact hearts. (c) The azide-incorporated hearts are isolated and lysed. The tissue lysates are reacted with alkyne-biotin for enrichment of sialylated glycoproteins with streptavidin beads, followed by gel-based proteomic identification.

In contrast to molecular imaging of proteins, the imaging strategies based on genetically encoded tags are not applicable for visualizing glycans, because of the nongenetically encoded nature of glycan biosynthesis. Although lectins are useful for imaging glycans in cultured cells,<sup>20,21</sup> they are not suited for labeling cardiac glycans in intact heart tissues, because lectins are not tissue-permeable. In fact, the limited tissue permeability of lectins has been exploited for staining the vasculatures.<sup>22</sup> Alternatively, the recently emerged chemical reporter strategy, termed metabolic glycan labeling, has shown promise for *in vivo* glycan imaging.<sup>23,24</sup> In this methodology, sugar analogues containing a bioorthogonal functional group or a chemical reporter (e.g., the azide) are incorporated into cell-surface glycans via the cell's own metabolic machinery. The azide serves as a chemical handle for subsequent coupling with fluorescent probes bearing a complementary bioorthogonal functional group. With application of the metabolic glycan labeling technique, *in vivo* visualization of cell-surface sialic acid,<sup>25</sup> *N*-acetylgalactosamine (GalNAc)  $\alpha$ -linked to serine or threonine, which is characteristic of mucin-type O-linked glycans,<sup>26</sup> and fucose<sup>27</sup> have been demonstrated in zebrafish. The glycome of *Caenorhabditis elegans*, another relatively simple organism, is also tractable to study by metabolic labeling and imaging with azidosugars.<sup>28,29</sup> However, glycan imaging in rodents has proven more challenging. Pioneering work by the Bertozzi group showed that azidosugars could be metabolized in living mice and detected *ex vivo*.<sup>30,31</sup> The Brindle group recently demonstrated *in vivo* imaging of tumor-associated glycans by employing two sequential bioorthogonal reactions to overcome the high background problem associated with labeling using one reaction.<sup>32</sup>

Herein we report the *in vivo* metabolic labeling of cardiac glycome in rats, which enables visualization of cardiomyocyte cell-surface glycans in intact hearts. Sialylated glycans and O-linked glycans were imaged by confocal fluorescence microscopy with high spatial resolution and found to distribute on cell membranes including cell–cell junctions and T-tubules.

Upon administering isoprenaline (ISO), a  $\beta$ -agonist clinically used for bradycardia and heart block, to the animals, we found that the upregulation of cell-surface sialylation is associated with cardiac hypertrophy. Furthermore, by conjugating the chemical reporter with an affinity tag, we performed proteomic analysis of cardiac sialylglycoproteins in the healthy and hypertrophic hearts. We identified more than 200 cardiac sialylated glycoproteins, and quantitative proteomic analysis revealed multiple sialylated proteins including neural cell adhesion molecule 1 (NCAM1), T-kininogens, and  $\alpha_2$ -macroglobulin ( $\alpha_2\text{M}$ ) that were upregulated during hypertrophy. Our results revealed the implication of sialylation in cardiac physiology and pathology.

## RESULTS AND DISCUSSION

***In Vivo* Metabolic Incorporation of Azidosugars into Rat Hearts.** We first tested the metabolic labeling of cardiac glycans in living rats, one of the predominant animal models currently used for cardiovascular diseases.<sup>33</sup> Based on the importance of sialic acids in cardiac function, we employed peracetylated *N*-azidoacetylmannosamine ( $\text{Ac}_4\text{ManNAz}$ )<sup>34</sup> to metabolically label the cardiac sialylated glycans. Using dosages similar to those used in mice,<sup>30</sup> we administered  $\text{Ac}_4\text{ManNAz}$  by intraperitoneal injection to Sprague–Dawley rats daily for 7 days (Figure 1). In living rats,  $\text{Ac}_4\text{ManNAz}$  passively diffused into the cells, where it was deacetylated by intracellular promiscuous esterases. The resulting ManNAz was metabolically converted to the corresponding azido sialic acid (SiaNAz), which was then incorporated into the sialylated glycans. We evaluated the *in vivo* metabolic incorporation of SiaNAz by reacting the lysates of heart tissues with alkyne-biotin using copper(I)-catalyzed azide–alkyne cycloaddition (CuAAC) assisted by the ligand BTAA.<sup>35</sup> Anti-biotin Western blot analysis of the  $\text{Ac}_4\text{ManNAz}$ -treated lysates showed that a wide repertoire of cardiac glycoproteins were metabolically labeled with SiaNAz (Figure S1 in Supporting Information).

We further characterized the azide-labeled sialylated glycans on the primary cardiomyocytes acutely isolated on the eighth day after  $\text{Ac}_4\text{ManNAz}$  administration. The isolated cells were reacted with alkyne-Fluor 488 using BTAA-assisted CuAAC and imaged by confocal fluorescence microscopy (Figure 1a and Figure 2). Cardiomyocytes from rats treated with

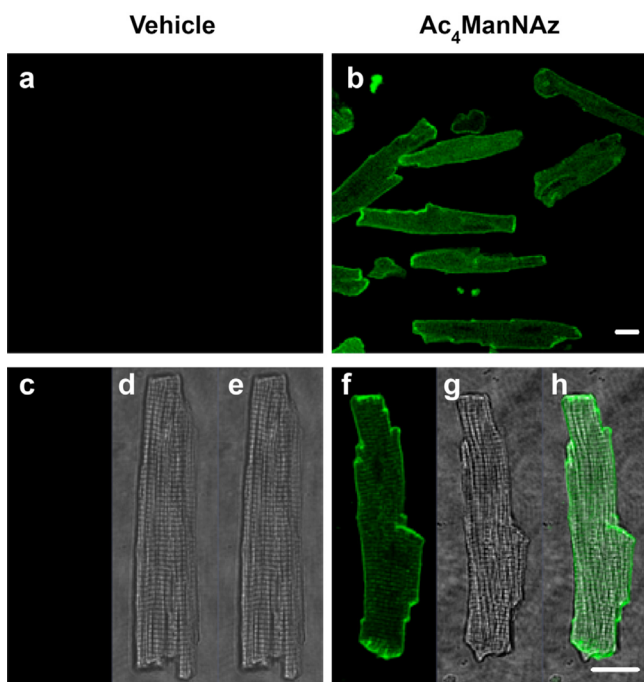


**Figure 2.** Metabolic labeling of sialylated glycoconjugates on primary rat cardiomyocytes. The cells were freshly isolated from rats treated with  $\text{Ac}_4\text{ManNAz}$  for 7 d. The cells were reacted with alkyne-Fluor 488 and imaged by confocal microscopy. (a,b) Fluorescence images of the isolated cardiomyocytes cultured on laminin. (c–h) Zoom-in view of a single cardiomyocyte, shown in fluorescence (c, f), DIC (d, g), and merged images (e, h). Scale bars: 20  $\mu\text{m}$ .

$\text{Ac}_4\text{ManNAz}$  exhibited significant cell-surface fluorescence, corresponding to the cell-surface sialylglycoconjugates (Figure 2b,f). Only negligible background fluorescence was observed in cardiomyocytes isolated from vehicle-treated rats (Figure 2a,c). These results confirm that  $\text{Ac}_4\text{ManNAz}$  is metabolized to

SiaNAz and incorporated into cardiac sialylated glycans in living rats, prompting us to image glycans in the intact hearts.

**Effects of Azidosugar Incorporation on the Cardiac Functions.** Before performing imaging experiments at the intact organ level, we asked whether the metabolic incorporation of  $\text{Ac}_4\text{ManNAz}$  would affect the cardiac functions of the animals. Echocardiographic measurements were performed on  $\text{Ac}_4\text{ManNAz}$ - and vehicle-administrated rats. No significant difference was observed between azidosugar- and vehicle-treated rats for all parameters measured (Figure S2 in Supporting Information). In addition, the isolated cardiomyocytes from azide-incorporated rats also exhibited normal excitation-contraction coupling (Figure S3 in Supporting Information). These results indicate that the metabolic incorporation of azidosugars does not cause apparent perturbations to cardiac functions.

**Confocal Imaging of Cell-Surface Sialylated Glycans in Intact Rat Hearts.** We next sought to perform the *in situ* imaging of the cardiac glycome in intact hearts using the Langendorff perfusion system, an experimental setup commonly used for studying heart functions in basic and preclinical research.<sup>36</sup> The optimized Langendorff system permits optical imaging of heart tissues over the course of several hours, without the complications involved in whole-animal experimentation.<sup>37</sup> More importantly, imaging of cardiac glycans in intact hearts avoids possible impairment of cell-surface glycan structures and biased loss of cardiomyocyte cells during enzymatic isolation of cardiomyocytes, as performed in Figures 1a and 2. We reasoned that the bioorthogonal reactions could be executed in the Langendorff-perfused hearts, after the *in vivo* metabolic labeling (Figure 1b). Toward this goal, we first chose to test the strain-promoted azide–alkyne cycloaddition or copper-free click chemistry to avoid the potential toxicity of copper.<sup>38–41</sup> After administration with  $\text{Ac}_4\text{ManNAz}$  for 7 days, the rats were euthanized, and the hearts were isolated and perfused on the Langendorff system with Tyrode's solution containing 50  $\mu\text{M}$  azido-dibenzocyclooctyne-Fluor 488 (DBCO-F488) (Figure 3a). After 20 min, the excess DBCO-F488 was washed by perfusing with Tyrode's solution, followed by imaging of the hearts by confocal fluorescence microscopy. Robust fluorescence was observed in the  $\text{Ac}_4\text{ManNAz}$ -treated hearts (Figure 3b). The fluorescence signal mostly distributed on cell surfaces and clearly demarcated cardiomyocytes, which

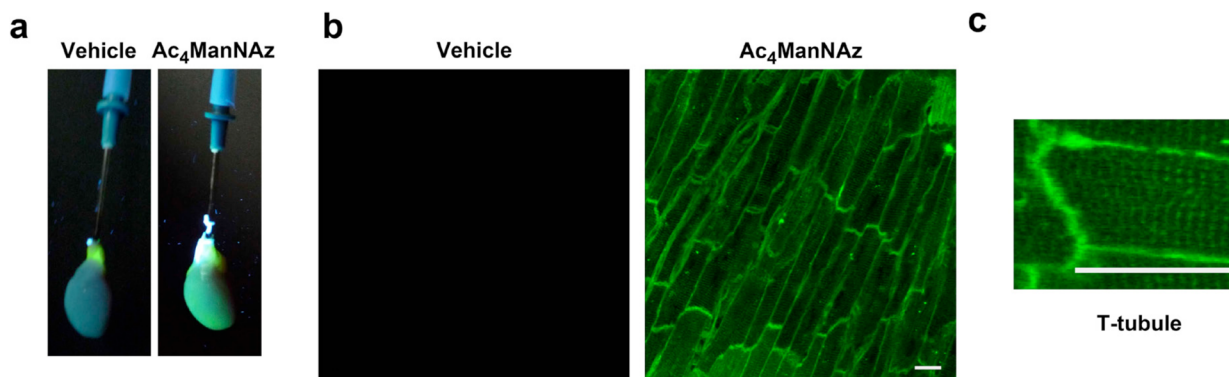


**Figure 3.** Imaging of cardiac glycans in intact rat hearts. (a) Photos of Langendorff-perfused hearts from rats treated with vehicle and  $\text{Ac}_4\text{ManNAz}$  followed by bioorthogonal labeling with DBCO-F488 under UV illumination. Note the green fluorescence of the  $\text{Ac}_4\text{ManNAz}$ -treated heart. (b) Confocal fluorescence images of azide-incorporated sialylated glycans in intact hearts that were isolated and perfused, followed by the reaction with DBCO-F488 using copper-free click chemistry. (c) Zoom-in view of the SiaNAz-labeled glycans in intact hearts, showing the structure of the T-tubule system. Scale bars: 20  $\mu\text{m}$ .

is in agreement with the cell-surface residence of sialylated glycans. Intense fluorescence signal on cell surfaces appeared more pronounced at the cell–cell contacts, revealing the sialylated glycans in cell–cell junctions. We observed virtually no background fluorescence in vehicle-treated hearts, indicating that the observed DBCO-F488 signal was attributed to the cell-surface glycans labeled by SiaNAz.

Since the ligand BTTAA was reported to curb the toxicity of CuAAC in cell culture and in zebrafish,<sup>35</sup> we tested its applicability in the perfused rat hearts. We successfully labeled the Ac<sub>4</sub>ManNAz-treated hearts using BTTAA-assisted CuAAC with no significant toxicity observed (Figure S4 in Supporting Information). Though promising, we believe more rigorous toxicity studies are needed. In this work, we employed the copper-free click chemistry for most experiments performed in the intact hearts.

#### Visualization of Sialylated Glycans on the T-tubules.

The azide-incorporated sialylated glycans were observed on the transverse tubule (T-tubule) network (Figure 3c). The T-tubules are the orderly spaced invaginations of cell surface membrane along Z-lines, which play an essential role in synchronizing cell-wide excitation and excitation–contraction coupling.<sup>42</sup> Our results indicate that the T-tubules contain sialylated glycans and the glycans are actively synthesized, during which the azidosugars are metabolically incorporated. Furthermore, the successful imaging of sialylated glycans on T-tubules demonstrates the high spatial resolution of our imaging method.

**Two-Color Imaging of Azide-Labeled Glycans and Lectin-Stained Vessels.** Our methodology enables, for the first time, direct imaging of membrane-associated glycans of myocytes in intact rat hearts. By contrast, antibodies and lectins are not applicable due to the poor tissue permeability. When lectins are applied into bloodstream, they cannot penetrate the vessels and therefore only stain the glycans on the epithelial cells of the vessel walls. Lectin staining has been commonly employed for imaging the vasculature.<sup>52</sup> To further demonstrate the advantages of our method, we sought to visualize simultaneously the cardiac glycans and blood vessels using two-color fluorescent imaging. We first applied tetramethylrhodamine (TRITC)-conjugated *Sambucus nigra* lectin (SNA), a lectin recognizing sialylated glycans, to the Langendorff-perfused hearts. The cardiac vasculature was clearly visualized using lectin staining (Figure S5 in Supporting Information). As expected, lectins did not stain cardiomyocytes. We then performed a two-color imaging experiment, where lectin perfusion was simultaneously applied with metabolic glycan labeling. The capillaries were clearly visualized by lectin staining, while the cell-surface sialylated glycans on myocytes were only imaged by metabolic labeling with Ac<sub>4</sub>ManNAz followed by bioorthogonal conjugation with DBCO-F488 (Figure 4).

**Upregulation of the Cardiac Glycan Biosynthesis during Cardiac Hypertrophy.** Having established the methodology for the visualization of cardiac glycome, we next applied it to probe the dynamic glycosylation during pathogenesis such as cardiac hypertrophy. Cardiac hypertrophy is initiated as an adaptive response of the heart to hemodynamic overload but often progresses to cardiac dysfunction and heart failure, which is one of the major causes of death worldwide.<sup>43</sup> Metabolic changes including altered fatty acid and glucose metabolism that accompany cardiac hypertrophy have been extensively investigated.<sup>44–48</sup> In contrast, the implication of the

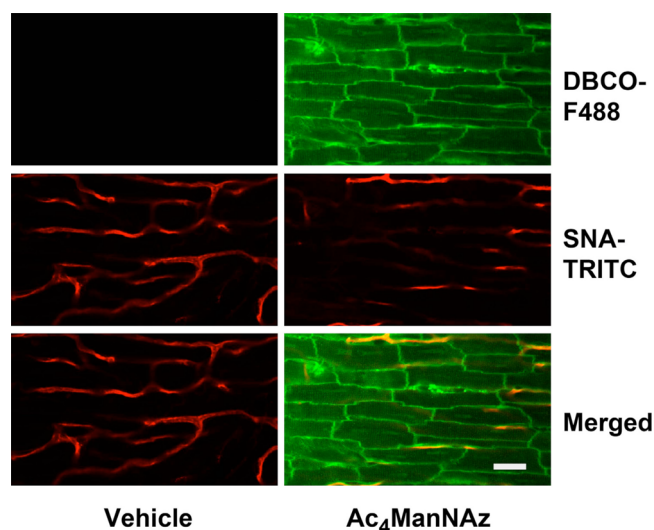


**Figure 4.** Two-color confocal fluorescence imaging of azide-labeled sialylated glycans and lectin-stained vessels. The fluorescence labeling was performed on Langendorff-perfused hearts after the rats were treated with Ac<sub>4</sub>ManNAz. TRITC-conjugated SNA was used to stain the vasculature of Ac<sub>4</sub>ManNAz-treated rat hearts. DBCO-F488 was used to chemically label azides. Scale bar: 20  $\mu$ m.

glycosylation pathways, which are coupled with glucose metabolism, remains poorly understood. Recently, augmented O-GlcNAc modification was observed in hypertrophic and failing hearts and was shown to be triggered by the unfolded protein response.<sup>49–52</sup> In this work, we sought to investigate sialylation during cardiac hypertrophy.

Cardiac hypertrophy can be induced by chronic administration of ISO,<sup>53</sup> a  $\beta$ -adrenoceptor agonist that is in clinical use for treating bradycardia and atrioventricular block. The ISO-induced hypertrophy model in rats has been commonly used for investigating the important genes and pathways involved in hypertrophy.<sup>54</sup> ISO or the saline control was injected to rats at 150 mg/kg per day for 7 days together with Ac<sub>4</sub>ManNAz or DMSO vehicle. The development of hypertrophy was monitored by M-mode echocardiography in living animals and further verified by histological sections of the isolated hearts. Cardiac hypertrophy, indicated by the apparent increase in heart size, heart weight/body weight ratio, left ventricular posterior wall thickness, and cardiac contractility in ISO-treated rats, was successfully induced without interference from azidosugar administration (Figure 5a,b, and Figure S6 in Supporting Information). In Ac<sub>4</sub>ManNAz-administrated rats, ISO treatment resulted in a significant increase in fluorescence signals, suggesting the increase of newly synthesized sialylated glycans during the progression of cardiac hypertrophy (Figure 5c,d). To include cardiomyocytes residing in deeper tissues that were out of the penetration depth of the light into analysis, we acutely isolated cells from Ac<sub>4</sub>ManNAz-administrated rat hearts. Quantification of confocal images of isolated cardiomyocytes revealed a similar increase of newly synthesized sialylated glycans in cardiac hypertrophy (Figure S7 in Supporting Information). These results demonstrate that chronic ISO treatment results in an increase of the de novo biosynthesis of cell-surface sialylated glycans.

**Proteomic Analysis of Sialylated Glycoproteins in Healthy and Hypertrophic Hearts.** The overall increase in sialylglycoconjugate biosynthesis revealed in the imaging experiments prompted us to uncover the differences in

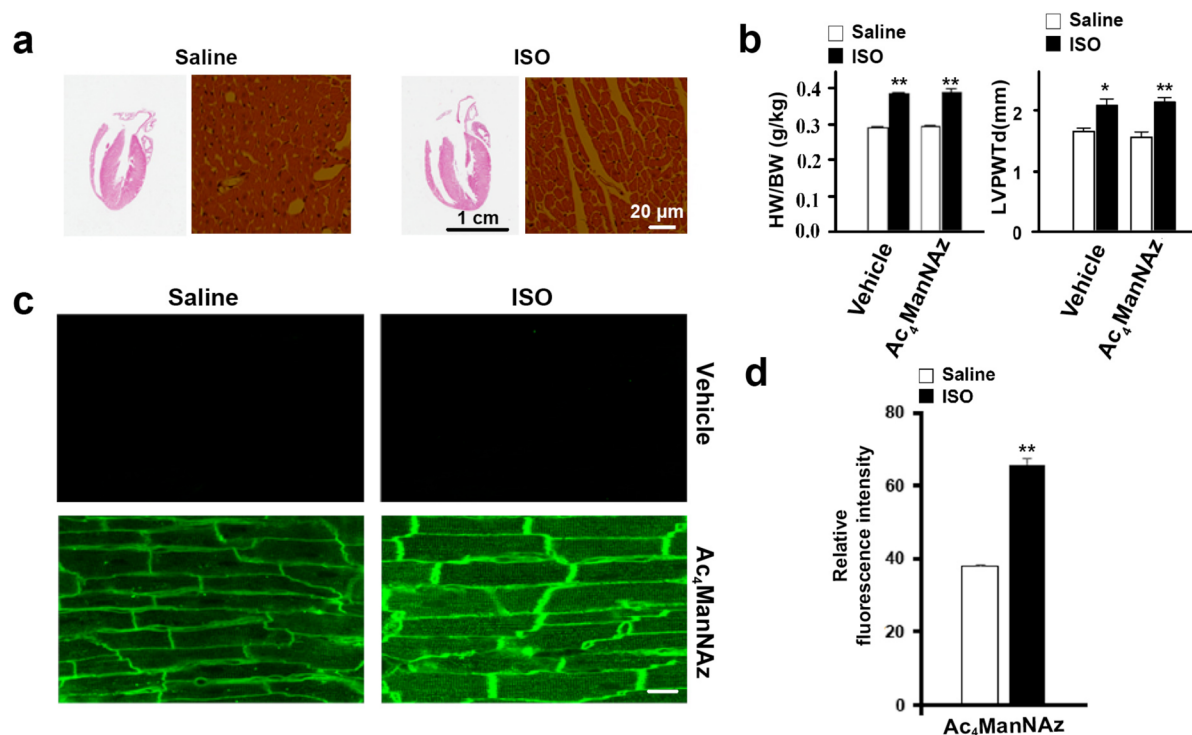


**Figure 5.** Upregulation of sialylation in cardiac hypertrophy. (a) Histological sections and hematoxylin and eosin (HE) staining of hearts from saline- and ISO-treated rats. (b) Heart weight/body weight ratio (HW/BW) and left ventricular posterior wall thickness at end diastole (LVPWTd) in control and ISO-treated rats. In the ISO-treated group, rats injected with vehicle and Ac<sub>4</sub>ManNAz exhibited significant increase in HW/BW and LVPWTd, indicating the development of cardiac hypertrophy. The HW/BW and LVPWTd were quantified by the M-mode echocardiography. Error bars represent the standard error of mean (SEM) from measurements from more than four rats. \**t* test  $P < 0.05$  between the saline and ISO-treated groups; \*\**t* test  $P < 0.01$  between the saline and ISO-treated groups. (c) Confocal fluorescence images of control and hypertrophy-induced hearts from rats injected with vehicle and Ac<sub>4</sub>ManNAz. DBCO-F488 was used to fluorescently label azide-incorporated sialylated glycans. All images were taken with a same exposure time. Scale bar: 20  $\mu$ m. (d) Quantification of relative fluorescence intensity resulting from sialylated glycans in control and hypertrophic hearts. Error bars represent the SEM from more than 100 measurements. \*\**t* test  $P < 0.01$  between the saline and ISO-treated groups.

sialylglycoprotein biosynthesis between healthy and hypertrophic hearts. We developed a glycoproteomic approach to enrich and identify cardiac sialylated glycoproteins (Figure 1c). Notably, our methodology should selectively identify the newly synthesized sialylated glycoproteins that are metabolically labeled with azidosugars. By comparison, enrichment of sialylated glycopeptides using titanium dioxide chromatography enabled proteomic identification of steady-state sialylated glycoproteins.<sup>12,55</sup> Therefore, the metabolic labeling method is well suited for probing the dynamic changes of sialylated proteome during hypertrophy.

Toward this goal, we administered Ac<sub>4</sub>ManNAz or vehicle to the saline- and ISO-treated rats for 7 days. After the metabolically labeled heart tissues were isolated and lysed, the tissue lysates were reacted with alkyne-biotin, followed by enrichment with streptavidin beads. Anti-biotin Western blot analysis showed much higher labeling intensity for glycoproteins from lysates of hypertrophic hearts, which is consistent with the imaging results (Figure 6a). The enriched glycoproteins were then subjected to gel-based proteomic identification by tandem mass spectrometry. Using a high-confidence filter (i.e., proteins were identified at least twice in three independent experiments with  $\geq 5$  spectral counts and  $\geq 5$ -fold increase above the vehicle-administered samples), we selectively identified 169 and 172 newly synthesized sialylated glycoproteins in the healthy and hypertrophic hearts, respectively (Figure 6b,c; Figure S8, Table S1a,b, and dataset

S1 in Supporting Information). Most of the identified proteins are either membrane or secreted proteins, containing the consensus sequence of N-linked glycosylation (N-X-S/T, where X is any amino acid except proline). Gene ontology analysis of the sialylated proteins revealed several biological processes enriched both in saline- and in ISO-treated samples, including response to wounding ( $P = 6.50 \times 10^{-22}$  and  $1.60 \times 10^{-19}$  in saline- and ISO-treated samples, respectively), cell adhesion ( $P = 1.00 \times 10^{-18}$ ,  $3.10 \times 10^{-19}$ ), and acute inflammatory response ( $P = 1.90 \times 10^{-13}$ ,  $4.90 \times 10^{-12}$ ) (modified Fisher's exact test) (Figure 6d and Figure S9 in Supporting Information).

In the high-confidence lists, 151 sialylated proteins were identified in both the healthy and hypertrophic hearts (Figure 6e). The 21 proteins uniquely identified in the hypertrophic hearts appeared either in the medium-confidence list (i.e., proteins were identified once in three independent experiments with  $\geq 5$  spectral counts and  $\geq 5$ -fold increase above the vehicle-administered samples; Table S2a in Supporting Information) or in the low-confidence list (Table S3a in Supporting Information) from the healthy hearts, and vice versa for the 18 proteins uniquely in the high-confidence list of the saline-treated rats (Table S2b and 3b in Supporting Information). For the total 190 sialylglycoproteins in the high-confidence list, relative abundance of individual proteins between the ISO- and saline-treatment conditions was assessed by spectral counting, that is, counting how many times a protein was identified by the fragmentation spectra of its peptides (Figure 6e).<sup>56,57</sup>

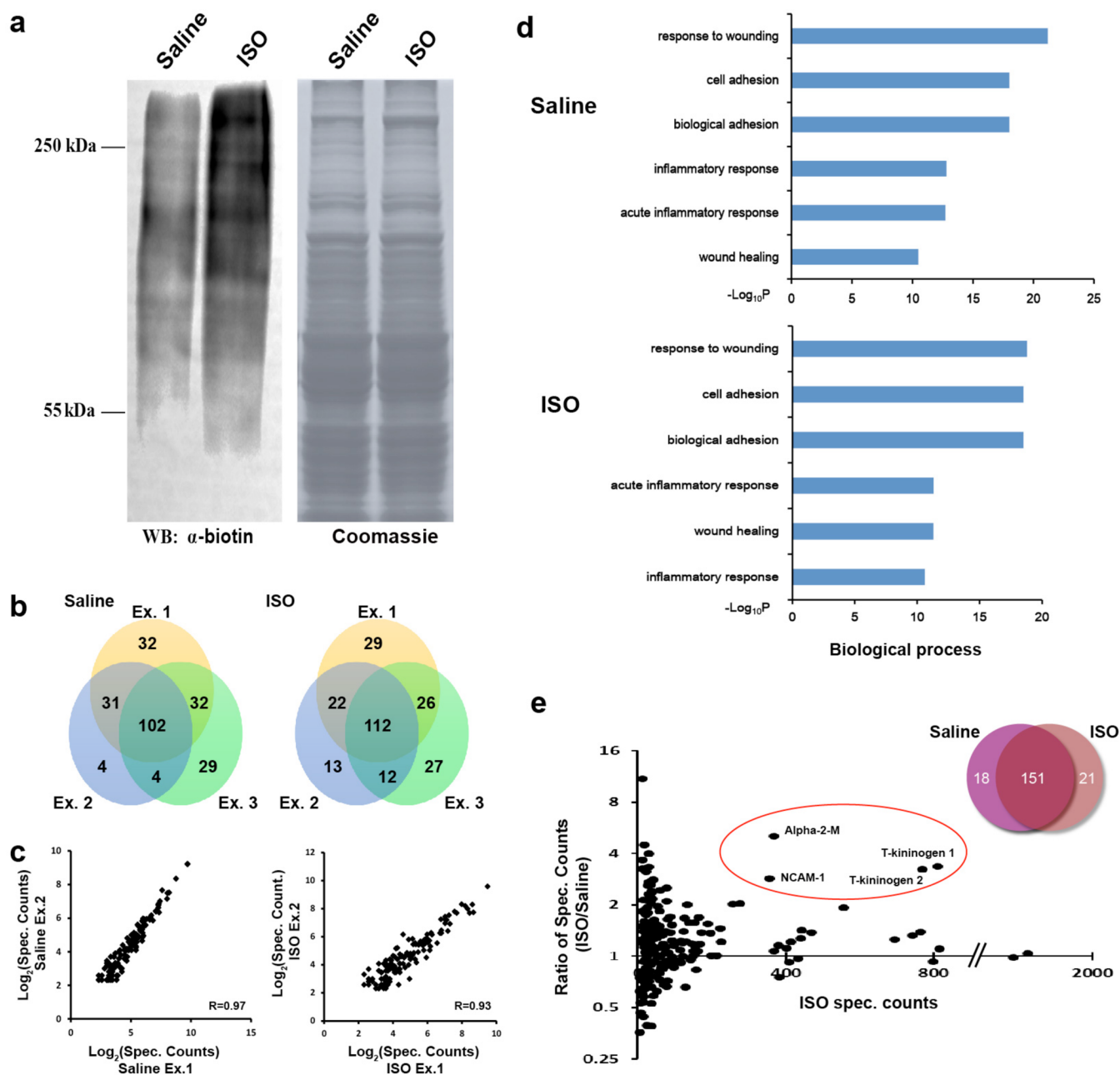


**Figure 6.** Proteomic analysis of sialyl glycoproteins in healthy and hypertrophic hearts. (a) The saline- and ISO-treated rats were administered Ac<sub>4</sub>ManNAz for 7 d. The azide-labeled heart tissues were isolated and lysed, followed by reaction with alkyne-biotin and enrichment using streptavidin beads. Antibiotin immunoblot (left panel) shows the enriched sialylated glycoproteins, and Coomassie blue staining (right panel) shows the input lysates before enrichment. The enriched glycoproteins were analyzed by gel-based proteomic identification using tandem mass spectrometry. (b) Overlap of identified sialylated proteins from three biological replicate experiments for saline- and ISO-treated hearts. (c) Pearson correlation plot for overlapping proteins from saline experiments (133 proteins, comparing experiment 1 with experiment 2) and ISO experiments ((134 proteins, comparing experiment 1 with experiment 2)). (d) Biological processes enriched in the newly synthesized sialylated glycoproteins identified in the saline- and ISO-treated hearts. The top six enriched processes are shown. (e) Relative changes of the biosynthesis of individual sialylated proteins between ISO- and saline-treated hearts. Spectral counting was used to access the relative abundance of individual proteins. Hits (190 in total) from both conditions were combined for this analysis. The proteins were sorted by the spectral counts in the ISO-treated samples (*x* axis).

Overall, a significant number of sialylated proteins exhibited upregulated biosynthesis in the hypertrophic hearts. The observed increase in spectral counts could be contributed by the upregulation of the biosynthesis at the protein level or the upregulation of protein sialylation. In this work, the upregulated biosynthesis of sialylated proteins was referred to as the total outcome of these two contributing factors hereafter. Among the

sialylated proteins identified with high spectral counts (Table S4 in Supporting Information), NCAM1, T-kininogens, and  $\alpha_2$ M were mostly upregulated (the inserted red circle in Figure 6e). NCAM1 has previously been reported to be upregulated in hypertrophic rats<sup>16</sup> and a genetic variation in NCAM1 was identified in hypertensive families.<sup>58</sup> The increased secretion of serum protein  $\alpha_2$ M has been shown to be involved in the

development of cardiac hypertrophy in rats.<sup>59,60</sup> Our glycoproteomic results not only support previous findings but also suggest the potential implications of sialylation of NCAM1 and  $\alpha_2$ M in hypertrophy. In addition, our results reveal a list of sialylated proteins whose upregulation during hypertrophy has not been well studied.

**Visualization of Cell-Surface Glycans in Rat Hearts Using Ac<sub>4</sub>GalNAz.** Finally, we sought to demonstrate the general applicability of our methodology for probing cardiac glycosylation. To do so, we administered peracetylated *N*-azidoacetylgalactosamine (Ac<sub>4</sub>GalNAz) to living rats using a similar procedure. Similar to Ac<sub>4</sub>ManNAz, Ac<sub>4</sub>GalNAz treatment did not perturb cardiac functions and the excitation–contraction coupling (Figures S2 and 3 in Supporting Information). Click-labeling of the lysates of heart tissues with alkyne-biotin, followed by anti-biotin Western blot analysis, revealed a wide repertoire of cardiac glycoproteins incorporated with azides (Figure S10a in Supporting Information). In contrast to Ac<sub>4</sub>ManNAz, the metabolic fate of Ac<sub>4</sub>GalNAz is more versatile. GalNAz is metabolically converted to UDP-GalNAz for incorporation into the mucin-type O-linked glycans. Besides, UDP-GalNAz can be epimerized to UDP-*N*-azidoacetylglucosamine (GlcNAz) via the cross talk between the GalNAc and GlcNAc salvage pathways.<sup>61</sup> The resulting UDP-GlcNAz labels intracellular O-linked  $\beta$ -*N*-acetylglucosamine (O-GlcNAc)-modified proteins. In addition, although Ac<sub>4</sub>GalNAz was reported to primarily label O-linked glycans among various types of cell-surface glycans,<sup>26,62</sup> there has been evidence indicating that UDP-GlcNAz may be incorporated into cell-surface GlcNAc-containing glycans such as N-linked glycans.<sup>63–65</sup> Thus, the glycoproteins revealed in Figure S10a in Supporting Information included mucin-type O-linked glycoproteins, intracellular O-GlcNAc-modified proteins, and likely some cell-surface N-linked glycoproteins. Cell-surface glycans metabolically labeled by Ac<sub>4</sub>GalNAz were visualized on cardiomyocytes acutely isolated from Ac<sub>4</sub>GalNAz-treated rats (Figure S10b in Supporting Information). Since alkyne-Fluor 488 is membrane impermeable and thus the CuAAC reaction only occurs outside the cell membrane, only cell-surface glycans and not intracellular O-GlcNAcylated proteins were fluorescently labeled in the Ac<sub>4</sub>GalNAz-treated cells. We reasoned that the observed fluorescence corresponded mainly to the mucin-type O-linked glycans, with a relatively small contribution from GlcNAc-containing cell-surface glycans.

Similarly, azide-incorporated cell-surface glycans were successfully imaged by confocal fluorescence microscopy in the perfused hearts, which were isolated after Ac<sub>4</sub>GalNAz administration, followed by conjugation with DBCO-F488 (Figure S11a in Supporting Information) or alkyne-488 using BTAA-assisted CuAAC (Figure S11b in Supporting Information). Moreover, we asked whether the bioorthogonal labeling could be performed in living animals (Figure S12a in Supporting Information). We intraperitoneally injected an Ac<sub>4</sub>GalNAz-administered rat with DBCO-F488 at a dosage of 0.16 mmol/kg. After 3 h, the rat was euthanized, and the heart was isolated, perfused on the Langendorff system, and imaged by laser scanning confocal microscopy. Imaging results similar to those by click-labeling in the perfused hearts were observed (Figure S12b in Supporting Information). Bioorthogonal labeling in living animals should enable *in vivo* imaging by using intravital microscopy.<sup>66–68</sup> It is also worth noting that performing bioorthogonal labeling in the isolated perfused

hearts is more economical in terms of the consumption of fluorescent reagents.

## CONCLUSION

Glycosylation plays an important functional role in mediating cardiac development and functions. As previously revealed by GeneChip microarray analysis and mass spectrometry profiling, glycone expression and glycome remodeling are significantly differentiated among neonatal and adult atrial and ventricular myocytes.<sup>4</sup> In cardiac pathogenesis such as hypertrophy, sugar metabolism is dramatically altered.<sup>44,45,52</sup> Although sialylation has been proven important for regulating the functions of various ion channels on cardiomyocytes,<sup>67,9,11</sup> the dynamic changes of the sialome during hypertrophy remains poorly characterized. Molecular imaging of glycans at the intact organ level holds great promise for elucidating the functional role of sialylation in cardiac pathogenesis but has been technically challenging.

Our approach exploiting the metabolic glycan labeling technique enables direct visualization of the dynamics of the biosynthesis of a specific subset of the cardiac glycome, such as the sialome and O-glycome, at the intact organ level. This method was used to probe the remodeling of the cardiac sialome during pathological processes, such as cardiac hypertrophy. Interestingly, we discovered that the biosynthesis of sialylated glycans is upregulated during the progression of cardiac hypertrophy. Importantly, the chemical reporter strategy also offers a platform for proteomic identification of the newly synthesized glycoproteins during hypertrophy. Our findings suggest the potential implication of sialylation in cardiac development and pathogenesis. Finally, this approach may be generally applicable to other tissues such as kidney, liver, and brain.

## ASSOCIATED CONTENT

### Supporting Information

Experimental procedures, supporting figures, proteomic data tables as described in the text. This material is available free of charge via the Internet at <http://pubs.acs.org>.

## AUTHOR INFORMATION

### Corresponding Authors

xingchen@pku.edu.cn  
wsq@pku.edu.cn  
jingzhao@nju.edu.cn

### Author Contributions

▽ J.R., J.H., and L.D. contributed equally to this work.

### Notes

The authors declare no competing financial interest.

## ACKNOWLEDGMENTS

We thank the mass spectrometry facility of National Center for Protein Sciences at Peking University for assistance with proteomic identification and Mr. W. Liu for assistance with graphics. This work was supported by the National Basic Research Program of China (973 Program) Grants 2012CB917303 to X.C. and 2011CB809101 to S.Q.W. and the National Natural Science Foundation of China Grants 91313301 and 21172013 to X.C. and 81370203 to S.Q.W.).

## REFERENCES

- (1) Comelli, E. M.; Head, S. R.; Gilmartin, T.; Whisenant, T.; Haslam, S. M.; North, S. J.; Wong, N.-K.; Kudo, T.; Narimatsu, H.; Esko, J. D.; Drickamer, K.; Dell, A.; Paulson, J. C. *Glycobiology* **2006**, *16*, 117.
- (2) Haltiwanger, R. S.; Lowe, J. B. *Annu. Rev. Biochem.* **2004**, *73*, 491.
- (3) Fuster, M. M.; Esko, J. D. *Nat. Rev. Cancer.* **2005**, *5*, 526.
- (4) Montpetit, M. L.; Stocker, P. J.; Schwetz, T. A.; Harper, J. M.; Norring, S. A.; Schaffer, L.; North, S. J.; Jang-Lee, J.; Gilmartin, T.; Head, S. R.; Haslam, S. M.; Dell, A.; Marth, J. D.; Bennett, E. S. *Proc. Natl. Acad. Sci. U.S.A.* **2009**, *106*, 16517.
- (5) Ngoh, G. A.; Facundo, H. T.; Zafir, A.; Jones, S. P. *Circ. Res.* **2010**, *107*, 171.
- (6) Ufret-Vincenty, C. A.; Baro, D. J.; Santana, L. F. *Am. J. Physiol.: Cell Physiol.* **2001**, *281*, C464.
- (7) Stocker, P. J.; Bennett, E. S. *J. Gen. Physiol.* **2006**, *127*, 253.
- (8) Anderson, C. L.; Delisle, B. P.; Anson, B. D.; Kilby, J. A.; Will, M. L.; Tester, D. J.; Gong, Q.; Zhou, Z.; Ackerman, M. J.; January, C. T. *Circulation* **2006**, *113*, 365.
- (9) Schwetz, T. A.; Norring, S. A.; Ednie, A. R.; Bennett, E. S. *J. Biol. Chem.* **2011**, *286*, 4123.
- (10) Chandrasekhar, K. D.; Lvov, A.; Terrenoire, C.; Gao, G. Y.; Kass, R. S.; Kobertz, W. R. *J. Physiol.* **2011**, *589*, 3721.
- (11) Norring, S. A.; Ednie, A. R.; Schwetz, T. A.; Du, D.; Yang, H.; Bennett, E. S. *FASEB J.* **2013**, *27*, 622.
- (12) Parker, B. L.; Palmisano, G.; Edwards, A. V. G.; White, M. Y.; Engholm-Keller, K.; Lee, A.; Scott, N. E.; Kolarich, D.; Hambly, B. D.; Packer, N. H.; Larsen, M. R.; Cordwell, S. J. *Mol. Cell. Proteomics* **2011**, *10*, No. M110.006833.
- (13) Crook, J. R.; Goldman, J. H.; Dalziel, M.; Madden, B.; McKenna, W. J. *Clin. Cardiol.* **1997**, *20*, 455.
- (14) Jaeken, J.; Matthijs, G. *Annu. Rev. Genomics Hum. Genet.* **2007**, *8*, 261.
- (15) Kiarash, A.; Kelly, C. E.; Phinney, B. S.; Valdivia, H. H.; Abrams, J.; Cala, S. E. *Cardiovasc. Res.* **2004**, *63*, 264.
- (16) Kimura, K.; Ieda, M.; Kanazawa, H.; Yagi, T.; Tsunoda, M.; Ninomiya, S.-I.; Kurosawa, H.; Yoshimi, K.; Mochizuki, H.; Yamazaki, K.; Ogawa, S.; Fukuda, K. *Circ. Res.* **2007**, *100*, 1755.
- (17) Marth, J. D.; Grewal, P. K. *Nat. Rev. Immunol.* **2008**, *8*, 874.
- (18) Kolwicz, S. C.; Tian, R. *Cardiovasc. Res.* **2011**, *90*, 194.
- (19) Laflamme, M. A.; Murry, C. E. *Nat. Immunol.* **2011**, *473*, 326.
- (20) Carlsson, S.; Carlsson, M. C.; Leffler, H. *Glycobiology* **2007**, *17*, 906.
- (21) O-Uchi, J.; Komukai, K.; Kusakari, Y.; Obata, T.; Hongo, K.; Sasaki, H.; Kurihara, S. *Proc. Natl. Acad. Sci. U.S.A.* **2005**, *102*, 9400.
- (22) Debbage, P. L.; Griebel, J.; Ried, M.; Gneiting, T.; DeVries, A.; Hutzler, P. *J. Histochem. Cytochem.* **1998**, *46*, 627.
- (23) Laughlin, S. T.; Bertozzi, C. R. *Proc. Natl. Acad. Sci. U.S.A.* **2009**, *106*, 12.
- (24) Rouhanifard, S. H.; Nordström, L. U.; Zheng, T.; Wu, P. *Chem. Soc. Rev.* **2013**, *42*, 4284.
- (25) Dehnert, K. W.; Baskin, J. M.; Laughlin, S. T.; Beahm, B. J.; Naidu, N. N.; Amacher, S. L.; Bertozzi, C. R. *ChemBioChem* **2012**, *13*, 353.
- (26) Laughlin, S. T.; Baskin, J. M.; Amacher, S. L.; Bertozzi, C. R. *Science* **2008**, *320*, 664.
- (27) Soriano Del Amo, D.; Wang, W.; Jiang, H.; Besanceney, C.; Yan, A. C.; Levy, M.; Liu, Y.; Marlow, F. L.; Wu, P. *J. Am. Chem. Soc.* **2010**, *132*, 16893.
- (28) Laughlin, S. T.; Bertozzi, C. R. *ACS Chem. Biol.* **2009**, *4*, 1068.
- (29) Attreed, M.; Desbois, M.; van Kuppevelt, T. H.; Bülow, H. E. *Nat. Methods* **2012**, *9*, 477.
- (30) Prescher, J. A.; Dube, D. H.; Bertozzi, C. R. *Nature* **2004**, *430*, 873.
- (31) Dube, D. H.; Prescher, J. A.; Quang, C. N.; Bertozzi, C. R. *Proc. Natl. Acad. Sci. U.S.A.* **2006**, *103*, 4819.
- (32) Neves, A. A.; Stöckmann, H.; Wainman, Y. A.; Kuo, J. C.-H.; Fawcett, S.; Leeper, F. J.; Brindle, K. M. *Bioconjugate Chem.* **2013**, *24*, 934.
- (33) Zaragoza, C.; Gomez-Guerrero, C.; Martin-Ventura, J. L.; Blanco-Colio, L.; Lavin, B.; Mallavia, B.; Tarin, C.; Mas, S.; Ortiz, A.; Egido, J. *J. Biomed. Biotechnol.* **2011**, *2011*, No. 497841.
- (34) Saxon, E.; Bertozzi, C. R. *Science* **2000**, *287*, 2007.
- (35) Besanceney-Webler, C.; Jiang, H.; Zheng, T.; Feng, L.; Soriano Del Amo, D.; Wang, W.; Klivansky, L. M.; Marlow, F. L.; Liu, Y.; Wu, P. *Angew. Chem., Int. Ed.* **2011**, *50*, 8051.
- (36) Bell, R. M.; Mocanu, M. M.; Yellon, D. M. *J. Mol. Cell. Cardiol.* **2011**, *50*, 940.
- (37) Efimov, I. R.; Nikolski, V. P.; Salama, G. *Circ. Res.* **2004**, *95*, 21.
- (38) Agard, N. J.; Prescher, J. A.; Bertozzi, C. R. *J. Am. Chem. Soc.* **2004**, *126*, 15046.
- (39) Chang, P. V.; Prescher, J. A.; Sletten, E. M.; Baskin, J. M.; Miller, I. A.; Agard, N. J.; Lo, A.; Bertozzi, C. R. *Proc. Natl. Acad. Sci. U.S.A.* **2010**, *107*, 1821.
- (40) Ning, X.; Guo, J.; Wolfert, M. A.; Boons, G.-J. *Angew. Chem., Int. Ed.* **2008**, *47*, 2253.
- (41) Debets, M. F.; van Berkel, S. S.; Schoffelen, S.; Rutjes, F. P. J. T.; van Hest, J. C. M.; van Delft, F. L. *Chem. Commun.* **2010**, *46*, 97.
- (42) Brette, F.; Orchard, C. *Circ. Res.* **2003**, *92*, 1182.
- (43) Heineke, J.; Molkentin, J. D. *Nat. Rev. Mol. Cell. Biol.* **2006**, *7*, 589.
- (44) Christe, M. E.; Rodgers, R. L. *J. Mol. Cell. Cardiol.* **1994**, *26*, 1371.
- (45) Sambandam, N.; Lopaschuk, G. D.; Brownsey, R. W.; Allard, M. F. *Heart Failure Rev.* **2002**, *7*, 161.
- (46) Ingwall, J. S.; Weiss, R. G. *Circ. Res.* **2004**, *95*, 135.
- (47) Wu, F.; Zhang, J.; Beard, D. A. *Proc. Natl. Acad. Sci. U.S.A.* **2009**, *106*, 7143.
- (48) Sansbury, B. E.; DeMartino, A. M.; Xie, Z.; Brooks, A. C.; Brainard, R. E.; Watson, L. J.; Defilippis, A. P.; Cummins, T. D.; Harbeson, M. A.; Brittan, K. R.; Prabhu, S. D.; Bhatnagar, A.; Jones, S. P.; Hill, B. G. *Circ.: Heart Failure* **2014**, *7*, 634.
- (49) Watson, L. J.; Facundo, H. T.; Ngoh, G. A.; Ameen, M.; Brainard, R. E.; Lemma, K. M.; Long, B. W.; Prabhu, S. D.; Xuan, Y.-T.; Jones, S. P. *Proc. Natl. Acad. Sci. U.S.A.* **2010**, *107*, 17797.
- (50) Ngoh, G. A.; Watson, L. J.; Facundo, H. T.; Jones, S. P. *Amino Acids* **2011**, *40*, 895.
- (51) Facundo, H. T.; Brainard, R. E.; Watson, L. J.; Ngoh, G. A.; Hamid, T.; Prabhu, S. D.; Jones, S. P. *Am. J. Physiol.: Heart Circ. Physiol.* **2012**, *302*, H2122.
- (52) Wang, Z. V.; Deng, Y.; Gao, N.; Pedrozo, Z.; Li, D. L.; Morales, C. R.; Criollo, A.; Luo, X.; Tan, W.; Jiang, N.; Lehrman, M. A.; Rothermel, B. A.; Lee, A.-H.; Lavandero, S.; Mammen, P. P. A.; Ferdous, A.; Gillette, T. G.; Scherer, P. E.; Hill, J. A. *Cell* **2014**, *156*, 1179.
- (53) Leenen, F. H.; White, R.; Yuan, B. *Am. J. Physiol.: Heart Circ. Physiol.* **2001**, *281*, H2410.
- (54) Doggrell, S. A.; Brown, L. *Cardiovasc. Res.* **1998**, *39*, 89.
- (55) Larsen, M. R.; Jensen, S. S.; Jakobsen, L. A.; Heegaard, N. H. H. *Mol. Cell. Proteomics* **2007**, *6*, 1778.
- (56) Liu, H.; Sadygov, R. G.; Yates, J. R. *Anal. Chem.* **2004**, *76*, 4193.
- (57) Dong, M.-Q.; Venable, J. D.; Au, N.; Xu, T.; Park, S. K.; Cociorva, D.; Johnson, J. R.; Dillin, A.; Yates, J. R. *Science* **2007**, *317*, 660.
- (58) Arnett, D. K.; Meyers, K. J.; Devereux, R. B.; Tiwari, H. K.; Gu, C. C.; Vaughan, L. K.; Perry, R. T.; Patki, A.; Claas, S. A.; Sun, Y. V.; Broeckel, U.; Kardia, S. L. *Circ. Res.* **2011**, *108*, 279.
- (59) Rajamanickam, C.; Sakthivel, S.; Babu, G. J.; Lottspeich, F.; Kadenbach, B. *Basic Res. Cardiol.* **2001**, *96*, 23.
- (60) Padmasekar, M.; Nandigama, R.; Wartenberg, M.; Schlüter, K.-D.; Sauer, H. *Cardiovasc. Res.* **2007**, *75*, 118.
- (61) Boyce, M.; Carrico, I. S.; Ganguli, A. S.; Yu, S.-H.; Hangauer, M. J.; Hubbard, S. C.; Kohler, J. J.; Bertozzi, C. R. *Proc. Natl. Acad. Sci. U.S.A.* **2011**, *108*, 3141.
- (62) Hang, H. C.; Yu, C.; Kato, D. L.; Bertozzi, C. R. *Proc. Natl. Acad. Sci. U.S.A.* **2003**, *100*, 14846.
- (63) Luchansky, S. J.; Hang, H. C.; Saxon, E.; Grunwell, J. R.; Yu, C.; Dube, D. H.; Bertozzi, C. R. *Methods Enzymol.* **2003**, *362*, 249.

(64) Hubbard, S. C.; Boyce, M.; McVaugh, C. T.; Peehl, D. M.; Bertozzi, C. R. *Bioorg. Med. Chem. Lett.* **2011**, *21*, 4945.

(65) Zaro, B. W.; Yang, Y.-Y.; Hang, H. C.; Pratt, M. R. *Proc. Natl. Acad. Sci. U.S.A.* **2011**, *108*, 8146.

(66) Lehr, H. A.; Leunig, M.; Menger, M. D.; Nolte, D.; Messmer, K. *Am. J. Pathol.* **1993**, *143*, 1055.

(67) Looney, M. R.; Thornton, E. E.; Sen, D.; Lamm, W. J.; Glenny, R. W.; Krummel, M. F. *Nat. Methods* **2011**, *8*, 91.

(68) Lee, S.; Vinegoni, C.; Feruglio, P. F.; Fexon, L.; Gorbatov, R.; Pivoravov, M.; Sbarbati, A.; Nahrendorf, M.; Weissleder, R. *Nat. Commun.* **2012**, *3*, No. 1054.